A smooth interface method for simulating liquid crystal colloid dispersions

2004 J. Phys.: Condens. Matter 16 S1945

(http://iopscience.iop.org/0953-8984/16/19/007)

INSTITUTE OF PHYSICS PUBLISHING JOURNAL OF PHYSICS: CONDENSED MATTER

J. Phys.: Condens. Matter **16** (2004) S1945–S1955 PII: S0953-8984(04)72942-2

A smooth interface method for simulating liquid crystal colloid dispersions

Ryoichi Yamamoto[1], **Yasuya Nakayama and Kang Kim**

Department of Physics, Kyoto University, Kyoto 606-8502, Japan
and
PRESTO, Japan Science and Technology Agency, 4-1-8 Honcho, Kawaguchi, Saitama, Japan

E-mail: ryoichi@scphys.kyoto-u.ac.jp

Received 2 December 2003
Published 30 April 2004
Online at stacks.iop.org/JPhysCM/16/S1945
DOI: 10.1088/0953-8984/16/19/007

Abstract

A new method is presented for mesoscopic simulations of particle dispersions in liquid crystal solvents. It allows efficient first principle simulations of the dispersions involving many particles with many body interactions mediated by the solvents. Demonstrations have been performed for the aggregation of colloid dispersions in two dimensional nematic and smectic-C* solvents neglecting hydrodynamic effects, which will be taken into account in the near future.

1. Introduction

Dispersions of small particles in host fluids such as colloid suspensions and emulsions are of considerable technological importance and appear often in our everyday life as paints, foods, and drugs, for example. Many kinds of exotic interactions were found between particles mediated by the host fluids including screened Coulombic [1], depletion [1], fluctuation induced [2], and surface induced [3] forces. A striking example occurs when spherical particles are immersed in a liquid crystal (LC) solvent in the nematic phase [4]. For a single particle, the orientation of the solvent molecules is distorted due to the anchoring of the solvent molecules at the particle surface. Extensive studies have been done on this effect, and several characteristic configurations of the nematic field around a spherical particle have been identified [5–10]. When the strength of anchoring is increased so that normal anchoring is preferred, the solvent changes from quadrupolar to dipolar symmetries around the particle. When multiple particles are immersed in the solvent, long range anisotropic interactions are induced between particles due to elastic deformations of the nematic field [11–14]. The anisotropic interactions can have a pronounced effect not only on the local correlations of the particles [11], but also on their

[1] Author to whom any correspondence should be addressed.

phase behaviour [15–20] and on their mechanical properties [16]. It has been reported also that a similar, but somewhat different situation occurs when colloid particles are immersed in smectic-C* films [21–23].

The purpose of our project is to develop an efficient method suitable for simulating colloid dispersions immersed in LC solvents by using a smooth interface treatment of the colloid–solvent boundaries. While hydrodynamic effects are of great importance to these systems [24, 25], we omit them in the present paper. They will be taken into account in the near future also through the smooth interface [26]. The same method is applicable for charged colloid dispersions where the charge density on a colloid surface is given by a smooth function [27].

2. Mesoscopic model

Since analytical approaches for investigating complex materials such as the LC colloid dispersions considered here are extremely difficult, computer simulations are the most promising tool for investigating their static and dynamical properties. In colloid dispersions, the host fluid molecules are much smaller and move much faster than the dispersed particles. This enables us to use coarse grained mesoscopic variables, which should be described by the hydrodynamics, for the host fluids rather than treating them as fully microscopic objects [28, 29]. In the case of charged colloid suspensions for example, a mesoscopic method for the first principle simulations can be derived by treating the counter-ions as a charge density [30]. For the particle dispersions in LC solvents considered here, the mesoscopic free energy $\mathcal{F}$ of the system can be given by functionals of the director $\mathbf{n}(\mathbf{r})$, a common direction on which solvent molecules are aligned on average with a constraint $|\mathbf{n}(\mathbf{r})| = 1$, for a given particle configuration $\{\mathbf{R}_1 \cdots \mathbf{R}_N\}$:

$$\mathcal{F}(\mathbf{n}(\mathbf{r}); \{\mathbf{R}_1 \cdots \mathbf{R}_N\}) = \mathcal{F}_{\mathrm{el}} + \mathcal{F}_{\mathrm{s}} = \int \mathrm{d}\mathbf{r}\, f_{\mathrm{el}}(\mathbf{r}) + \oint \mathrm{d}S\, f_{\mathrm{s}}(S) \tag{1}$$

where

$$f_{\mathrm{el}}(\mathbf{r}) = \tfrac{1}{2}[K_1(\nabla \cdot \mathbf{n})^2 + K_2(\mathbf{n} \cdot \nabla \times \mathbf{n})^2 + K_3\{\mathbf{n} \times (\nabla \times \mathbf{n})\}^2] \tag{2}$$

is the Frank free energy [31] which represents the elastic energy density of the nematic solvent at $\mathbf{r}$ and the surface free energy

$$f_{\mathrm{s}}(S) = \frac{W}{2}[1 - (\mathbf{n} \cdot \boldsymbol{\nu})^2] \tag{3}$$

controls anchoring of the LC solvent at the surface element S of the particle. The coefficients K_1, K_2, and K_3 are the splay, twist, and bend elastic constants, respectively; and the single constant approximation ($K = K_1 = K_2 = K_3$) reduces equation (2) to the simpler form

$$f_{\mathrm{el}}(\mathbf{r}) = \frac{K}{2}[(\nabla \cdot \mathbf{n})^2 + (\nabla \times \mathbf{n})^2]. \tag{4}$$

W is the surface anchoring constant, and $\boldsymbol{\nu}$ is the unit vector normal to the colloid surface [7, 8]. The saddle-splay elastic term [8] is not considered here. The integral in the first term on the right-hand side of equation (1) runs over the whole solvent volume excluding the particles, and that in the second term runs over all solvent–particle interfaces. A simple scaling argument tells us $\mathcal{F}_{\mathrm{el}} \propto Ka^{d-2}$ and $\mathcal{F}_{\mathrm{s}} \propto Wa^{d-1}$ with a and d being the particle radius and the system dimension, respectively, thus the state of the dispersion should be controlled by the ratio $\mathcal{F}_{\mathrm{s}}/\mathcal{F}_{\mathrm{el}} \propto Wa/K$. Although this type of free energy functional is sufficient for single particle problems, it is not useful for simulating colloid dispersions involving many particles using molecular dynamics (MD) or Brownian type methods because the coupling

between solvent and the particles is given implicitly by limiting the integration space in both $\mathcal{F}_{\rm el}$ and $\mathcal{F}_{\rm s}$. This produces mathematical singularities at the interface when one calculates the force, $\mathbf{f}_n^{\rm PS} = -\partial\mathcal{F}/\partial\mathbf{R}_n$, acting on each particle mediated by the LC solvents. Calculation of the force is crucial for performing efficient simulations of many particle systems. Another serious problem of this type of functional is that in order to give correct boundary conditions at the particle–solvent interface, one has to use appropriate coordinates for performing grid-based numerical simulations rather than the usual Cartesian coordinates. This is generally difficult for particles with non-spherical shapes or for systems involving many particles even when each particle has a spherical shape. Also this makes use of the periodic boundary condition difficult, which is a fatal situation for simulating bulk materials.

To overcome these problems, we have modified equations (1), (3), and (4) by using a smooth interface between the solvent and the particles so that the coupling is given explicitly in the integrand through the interface [32]. The new free energy functional we propose has the form

$$\mathcal{F}(\mathbf{n}(\mathbf{r}); \{\mathbf{R}_1 \cdots \mathbf{R}_N\}) = \int \mathrm{d}\mathbf{r} \left[1 - \sum_{i=1}^{N} \phi_i(\mathbf{r})\right] f^{\rm el}(\mathbf{r}) + \int \mathrm{d}\mathbf{r} \sum_{i=1}^{N} \xi(\nabla\phi_i)^2 f_i^s(\mathbf{r}) \tag{5}$$

with

$$f^{\rm el}(\mathbf{r}) = \frac{K}{4R_{\rm c}^2} \tanh[R_{\rm c}^2(\nabla_\alpha(n_\beta n_\gamma))^2] \tag{6}$$

$$f_i^s(\mathbf{r}) = \frac{W}{2}\left[1 - \left(\frac{\nabla\phi_i}{|\nabla\phi_i|} \cdot \mathbf{n}\right)^2\right] \tag{7}$$

for nematic solvent and

$$f^{\rm el}(\mathbf{r}) = \frac{K}{2R_{\rm c}^2} \tanh[R_{\rm c}^2((\nabla \cdot \mathbf{n})^2 + (\nabla \times \mathbf{n})^2)] \tag{8}$$

$$f_i^s(\mathbf{r}) = W\left[1 - \frac{\nabla\phi_i}{|\nabla\phi_i|} \cdot \mathbf{n}\right] \tag{9}$$

for smectic-C* solvent. The summation convention is used for $\alpha, \beta, \gamma \in x, y, z$. The explicit form of the interfacial profile ϕ_n between dispersed particles and solvents and its spatial derivatives $\nabla_\alpha\phi_n$ are given by

$$\phi_n(\mathbf{r}) = \frac{1}{2}\left(\tanh\frac{a - |\mathbf{r} - \mathbf{R}_n|}{\xi} + 1\right) \tag{10}$$

and

$$\nabla_\alpha\phi_n(\mathbf{r}) = -\frac{r_\alpha - R_{n,\alpha}}{2\xi|\mathbf{r} - \mathbf{R}_n|} \cosh^{-2}\frac{a - |\mathbf{r} - \mathbf{R}_n|}{\xi} \tag{11}$$

respectively with the particle radius a and the interface thickness ξ. Note that the set of equations (5)–(11) reduces to equations (1), (3), and (4) for the limit $R_{\rm c}, \xi \to 0$. A similar idea for using a smooth interface was used to treat the hydrodynamic forces acting on particles dispersed in simple liquids [33], recently. For the nematic case, $f_{\rm el}$ is given by a function of a symmetric second rank tensor $q_{\alpha\beta} = n_\alpha n_\beta$ rather than the director $\mathbf{n}$ itself to take into account the symmetry of the nematic director $+\mathbf{n} \leftrightarrow -\mathbf{n}$ automatically. The semi-empirical functional form $(1/R_{\rm c}^2)\tanh[R_{\rm c}^2 \cdots]$ is applied in equations (6) and (8) to avoid the mathematical divergence of the elastic free energy density at the defect centres and to limit its value to $\Delta f_{\rm el} \sim K/R_{\rm c}^2$ and replace its core size with $R_{\rm c}$ as shown in figure 1. Another way to avoid the divergence would be to use the Landau–de Gennes type free energy with an order parameter $Q_{\alpha\beta}(\mathbf{r}) = Q(\mathbf{r})q_{\alpha\beta}(\mathbf{r})$, but this requires a prohibitively small lattice spacing near the defect points [34].

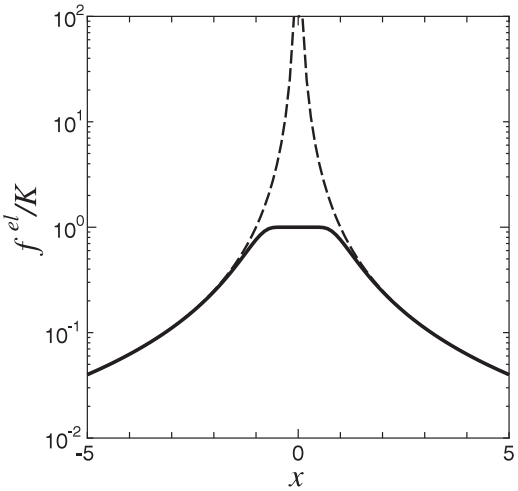

Figure 1. The elastic free energy density $f_{\rm el}(x)$ around a point defect at $x = 0$. The dashed curve is from equation (4), $f_{\rm el} \simeq K/x^2$, and the solid curve is from equation (6) or (8) with $R_{\rm c} = 1$, $f_{\rm el} \simeq K \tanh(1/x^2)$.

3. Numerical method

3.1. First principle simulation

The simulation procedure is as follows.

(i) For a given particle configuration $\{\mathbf{R}_1 \cdots \mathbf{R}_N\}$, obtain the interface profile $\phi_n(\mathbf{r})$ from equation (10). Then we can calculate the stable (or meta-stable) nematic configuration $\mathbf{n}^{(0)}(\mathbf{r})$ which should satisfy the equilibrium condition

$$\left.\frac{\delta \mathcal{F}}{\delta \mathbf{n}(\mathbf{r})}\right|_{\mathbf{n}(\mathbf{r})=\mathbf{n}^{(0)}(\mathbf{r})} = 0 \tag{12}$$

under the director constraint $|\mathbf{n}(\mathbf{r})| = 1$. One can perform this by numerical iterations such as the steepest descent or the conjugate gradient method. Although the time evolutions of $\mathbf{n}(\mathbf{r})$ should be determined by the hydrodynamic laws, we here assume $\mathbf{n}(\mathbf{r})$ follows adiabatically after $\{\mathbf{R}_1 \cdots \mathbf{R}_N\}$ for the sake of simplicity.

(ii) Once $\mathbf{n}^{(0)}(\mathbf{r})$ is obtained, the force acting on each particle mediated by the nematic solvents follows directly from the Hellmann–Feynman theorem

$$\mathbf{f}_n^{\rm PS}(\{\mathbf{R}_1 \cdots \mathbf{R}_N\}) \equiv -\left.\frac{\partial \mathcal{F}(\mathbf{n}(\mathbf{r}); \{\mathbf{R}_1 \cdots \mathbf{R}_N\})}{\partial \mathbf{R}_n}\right|_{\mathbf{n}(\mathbf{r})=\mathbf{n}^{(0)}(\mathbf{r})}. \tag{13}$$

The final forms are

$$\mathbf{f}_n^{\rm PS} = \frac{K}{4R_{\rm c}^2}\int {\rm d}\mathbf{r}\,\frac{\partial \phi_n}{\partial \mathbf{R}_n}\tanh[R_{\rm c}^2(\nabla_\alpha(n_\beta^0 n_\gamma^0))^2] + W\xi\int {\rm d}\mathbf{r}\,\frac{\partial(\nabla_\alpha\phi_n)}{\partial \mathbf{R}_n}(\nabla_\beta\phi_n)n_\alpha^0 n_\beta^0 \tag{14}$$

and

$$\mathbf{f}_n^{\rm PS} = \frac{K}{2R_{\rm c}^2}\int {\rm d}\mathbf{r}\,\frac{\partial \phi_n}{\partial \mathbf{R}_n}\tanh[R_{\rm c}^2((\nabla\cdot\mathbf{n}^0)^2 + (\nabla\times\mathbf{n}^0)^2)] + W\xi\int {\rm d}\mathbf{r}\,\frac{\partial(\nabla_\alpha\phi_n)}{\partial \mathbf{R}_n}\left[\frac{\nabla_\alpha\phi_n}{|\nabla\phi_n|}\nabla_\beta\phi_n n_\beta^0 + |\nabla\phi_n| n_\alpha^0\right] \tag{15}$$

in the cases of nematic and smectic-C* solvents, respectively. These forms are very convenient because one can compute both $\partial\phi_n/\partial\mathbf{R}_n$ and $\partial(\nabla_\alpha\phi_n)/\partial\mathbf{R}_n$ at any time since ϕ_n is an analytical function of $\mathbf{R}_n$.

(iii) Finally, update the particle positions according to appropriate equations of motion such as

$$m_n\frac{\mathrm{d}^2\mathbf{R}_n}{\mathrm{d}t^2} = \mathbf{f}_n^{\mathrm{PP}} + \mathbf{f}_n^{\mathrm{PS}} + \mathbf{f}_n^{\mathrm{H}} + \mathbf{f}_n^{\mathrm{R}} \tag{16}$$

where $\mathbf{f}_n^{\mathrm{PP}}$ is the force due to direct particle–particle interactions (hard or soft sphere for instance), $\mathbf{f}_n^{\mathrm{H}}$ and $\mathbf{f}_n^{\mathrm{R}}$ are the hydrodynamic and random forces. Repeating the steps (i)–(iii) enables us to perform first principles mesoscopic simulations for the dispersions containing many particles without neglecting many body interactions.

4. Results

4.1. Director configurations around a single particle

We have performed simple demonstrations for two dimensional (2D) LC colloid dispersions to test the performance of our procedure. The demonstration system has 100×100 lattice sites in a square box with a linear length $L = 100$. Other physical parameters are chosen rather arbitrarily as $R_c = 1$, $a = 5$, and $\xi = 2$, where the unit of length is the lattice spacing l. Since the director configurations in 2D can be expressed by a single scalar field $\theta(\mathbf{r})$, the tilt angle of the director against the horizontal (x-) direction, equation (12) then reduces to

$$\frac{\delta\mathcal{F}}{\delta\theta(\mathbf{r})} = \frac{\partial n_\alpha(\mathbf{r})}{\partial\theta(\mathbf{r})}\frac{\delta\mathcal{F}}{\delta n_\alpha(\mathbf{r})} = 0. \tag{17}$$

The boundary condition is fixed at $\theta(\mathbf{r}) = 0$ at the edge of the box to avoid rotations of the reference frame.

We first calculated the stable director configurations around a single particle immersed in 2D nematic and smectic-C* solvents and show them in figures 2(a) and (b), respectively. For the nematic solvent (a), the particle is accompanied by two $-1/2$ charge point defects with a strong anchoring condition $Wa/K = 4$. The distance between the defects and the particle centre is about $1.2a$, which is similar to the analytic value $1.236a$ [34], and the director configuration around the single particle possesses quadrupolar symmetry. This would correspond to the Saturn ring configuration observed in three dimensional (3D) systems. Although in principle particles can be accompanied by one -1 charge hedgehog defect in 2D as well as in 3D, such configurations are unstable in the present 2D system since the elastic penalty of having m point defects with charge c scales as mKc^2. This was directly confirmed by recent simulations with perfect normal anchoring [34] and also by our simulations. For the smectic-C* solvent (b) on the other hand, the particle is accompanied by one -1 charge point defect with an anchoring condition $Wa/K = 5$. The distance between the defect and the particle centre is about $1.4a$ which is again similar to the experimental value $1.4a \pm 0.1a$ [21] and the analytic one $\sqrt{2}a$ [23]. Note that the director configuration around the particle possesses dipolar symmetry similar to the experiment [21].

4.2. Aggregation of colloids in LC solvents

We have simulated the aggregation and ordering process of 30 and 10 colloid particles in nematic and smectic-C* solvents, respectively, after the isotropic to nematic or isotropic to smectic-C* transition occurred. Here we used the periodic boundary condition and set $Wa/K = 4$ (nematic) or 5 (smectic-C*). Other parameters are the same as in the

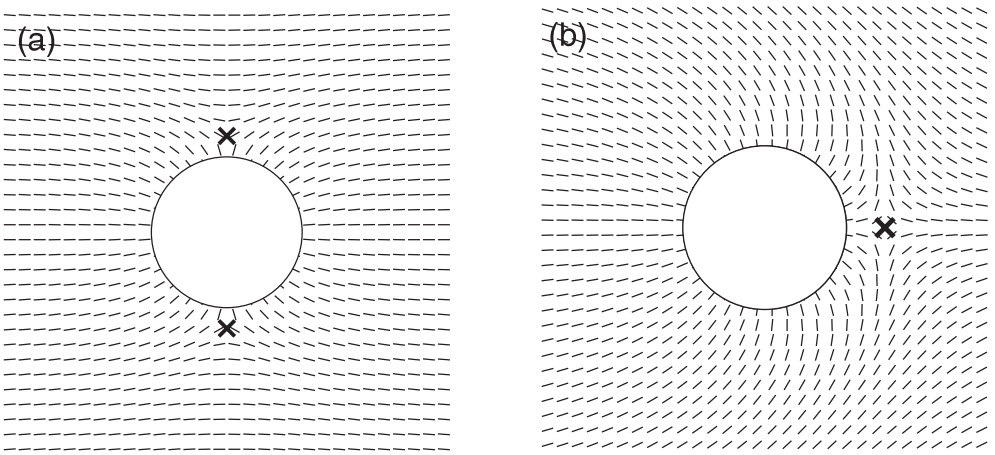

Figure 2. (a) The director configuration around a single particle immersed in nematic solvent with the strong anchoring condition $Wa/K = 4$. The crosses show two $-1/2$ charge point defects and the configuration obtained has a quadrupolar character. (b) The director configuration around a single particle immersed in smectic-C* solvent with $Wa/K = 5$. The cross shows a -1 charge point defect and the configuration obtained has a dipolar character. The white discs indicate the colloid particles. Only 9% of the total system is shown for display purposes.

previous single particle case. The simulation was performed starting from a random particle configuration which is a typical configuration when the solvent is in the isotropic phase ($K = 0$). We then set $K = 1$ and calculated $\mathbf{f}_n^{\mathrm{PS}}$ according to the present procedure. The particle configurations were updated by numerically solving the steepest descent equation,

$$\zeta \frac{\mathrm{d}\mathbf{R}_n}{\mathrm{d}t} = \mathbf{f}_n^{\mathrm{PS}} + \mathbf{f}_n^{\mathrm{PP}} \tag{18}$$

which is obtained by simply substituting $\mathrm{d}^2\mathbf{R}_n/\mathrm{d}t^2 = 0$, $\mathbf{f}_n^{\mathrm{R}} = 0$, and $\mathbf{f}_n^{\mathrm{H}} = -\zeta\,\mathrm{d}\mathbf{R}_n/\mathrm{d}t$ in equation (16). $\zeta = 1$ is a friction constant and thus the off-diagonal components of the hydrodynamic interaction were not considered. Here we obtain

$$\mathbf{f}_n^{\mathrm{PP}} = -\frac{\partial E_{\mathrm{PP}}}{\partial \mathbf{R}_n} \tag{19}$$

from the repulsive part of the Lennard-Jones potential,

$$E_{\mathrm{PP}} = 0.4 \sum_{n=1}^{N-1} \sum_{m=n+1}^{N} \left[\left(\frac{2a}{|\mathbf{r}_n - \mathbf{r}_m|} \right)^{12} - \left(\frac{2a}{|\mathbf{r}_n - \mathbf{r}_m|} \right)^{6} + \frac{1}{4} \right] \tag{20}$$

truncated at the minimum distance $|\mathbf{r}_n - \mathbf{r}_m| = 2^{7/6}a$, to avoid the particles overlapping each other within the colloid radius $\simeq a$. Snapshots from the present simulation are shown in figures 3 and 4 for dispersions in nematic and smectic-C* solvents, respectively. In figure 3, the particles are forming ordered clusters due to the quadrupolar attractive interaction among them. In figure 4 on the other hand, the particles are forming string-like clusters due to the dipolar attractive interaction among them. Similar results have been obtained recently by experiments [21]. Note that only up to two particle simulations have been done so far [8] and simulations of more than two particles would be extremely difficult or almost impossible even for 2D systems by means of other methods proposed previously.

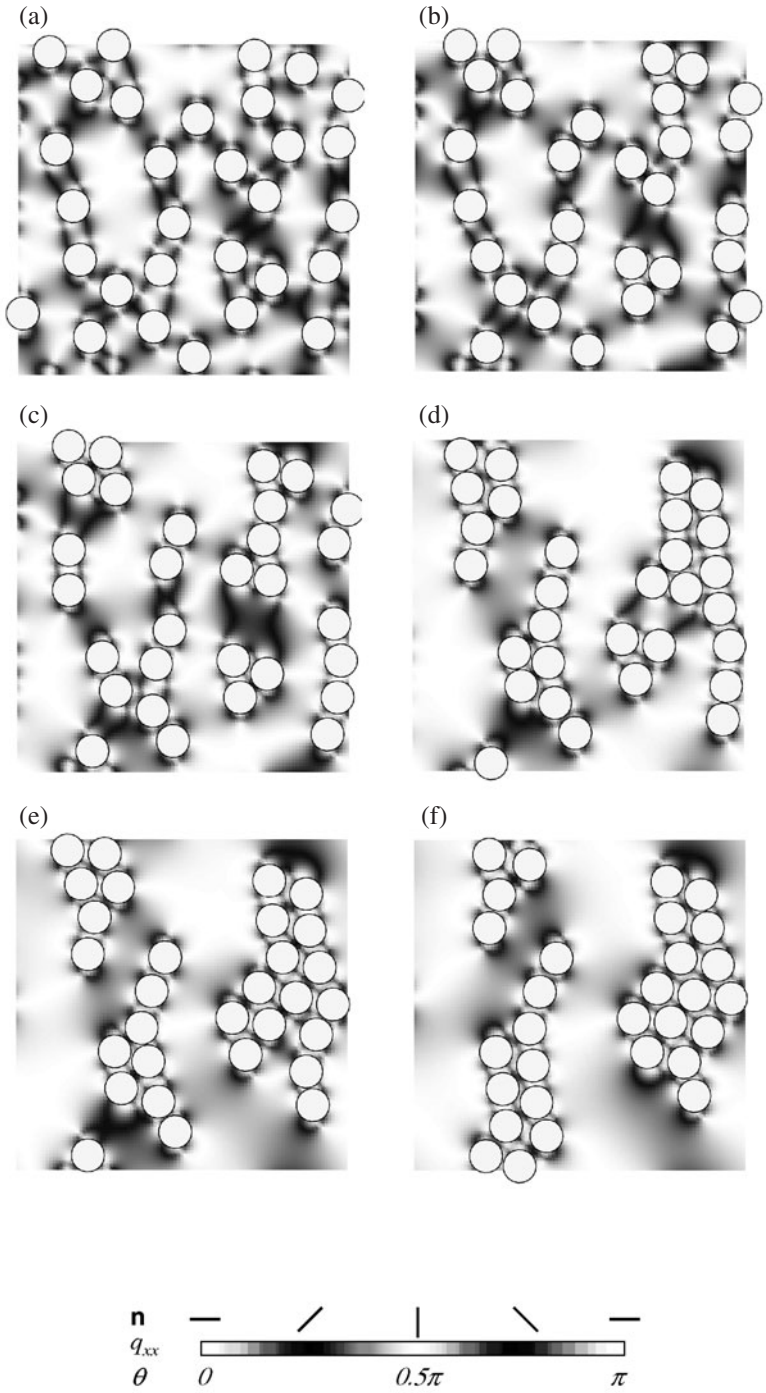

Figure 3. The aggregation and ordering process of colloid particles after the solvent exhibits the isotropic ($K = 0$) to nematic ($K = 1$) phase transition; (a) $t = 0$, (b) $t = 0.4$, (c) $t = 1.6$, (d) $t = 6.4$, (e) $t = 16$, and (f) $t = 40$. Each particle is accompanied by two $-1/2$ charge point defects. Darkness represents the value of q_{xx}^2. Black and white correspond to $q_{xx}^2 = 0$ and 0.25, respectively. They correspond also to $\theta = 0.25\pi, 0.75\pi$ and $0, 0.5\pi, \pi$ as shown in the gradation map.

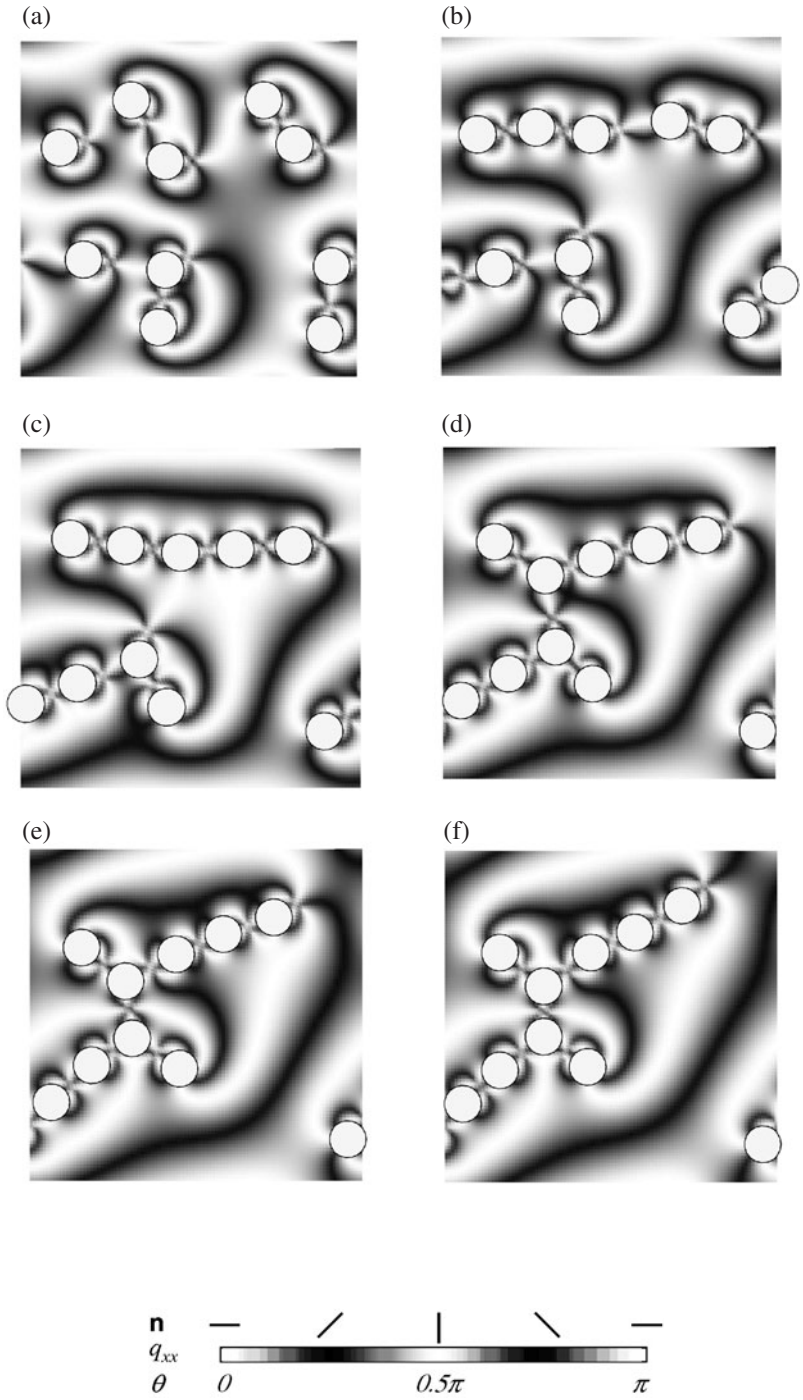

Figure 4. The aggregation and ordering process of colloid particles after the solvent exhibits the isotropic ($K = 0$) to smectic-C* ($K = 1$) phase transition; (a) $t = 0$, (b) $t = 0.25$, (c) $t = 1$, (d) $t = 4$, (e) $t = 10$, (f) $t = 25$. Each particle is accompanied by one -1 charge point defect. Darkness represents the value of q_{xx}^2. Black and white correspond to $q_{xx}^2 = 0$ and 0.25, respectively. They correspond also to $\theta = 0.25\pi, 0.75\pi$ and $0, 0.5\pi, \pi$ as shown in the gradation map.

5. Concluding remarks

In summary, we have developed a powerful simulation method for investigating colloid dispersions interacting via solvents. We proposed a free energy functional which is suitable for MD type simulations. The following modifications have been made to the original Frank free energy functional.

(i) The coupling between the LC solvents and particles at the interfaces is introduced explicitly through a smooth interface so that we can analytically calculate the force acting on each particle mediated by the host by taking derivatives of the free energy according to the particle positions.
(ii) The value of the free energy density is bounded semi-empirically to avoid a mathematical divergence in the defect centres.

We have performed demonstrations for 2D dispersions and confirmed that the method works quite well for systems which contain topological defects. Applications of this method to 3D systems should have no theoretical difficulties, but require somewhat heavier computation. This should allow the simulation of the chaining of the particles caused by the possible dipolar symmetry of the nematic configurations around a single particle. Although we have given only simple demonstrations of the method by performing simulations of the 2D system in this paper, simulations with physically more interesting situations such as systems with non-circular particles, asymmetric particle pairs with different particle size, or particles with non-normal anchoring as well as more realistic simulations in 3D systems are possible. Efforts at taking into account the hydrodynamic effects are now under way, by using smooth interface instead of imposing hydrodynamic boundary conditions at the colloid interface.

Acknowledgments

RY thanks Professors J-P Hansen, H Löwen, and Dr E Terentjev for helpful discussions. A part of the present calculation was carried out at the Human Genome Centre, Institute of Medical Science, University of Tokyo.

Appendix A. Numerical implementation for 2D nematic

Here, the superscripts i, j $(= 1, 2, \ldots, L)$ denote positions on a 2D lattice $(L \times L)$.

$$\mathcal{F}_{\mathrm{el}} = \frac{K}{4R_{\mathrm{c}}^2} \sum_{i,j} \left(1 - \sum_{n=1}^{N} \phi_n^{i,j} \right) \tanh \epsilon^{i,j} \tag{A.1}$$

$$\epsilon^{i,j} = \frac{R_{\mathrm{c}}^2}{2l^2} [(q_{\alpha\beta}^{i,j} - q_{\alpha\beta}^{i-1,j})^2 + (q_{\alpha\beta}^{i+1,j} - q_{\alpha\beta}^{i,j})^2 + (q_{\alpha\beta}^{i,j} - q_{\alpha\beta}^{i,j-1})^2 + (q_{\alpha\beta}^{i,j+1} - q_{\alpha\beta}^{i,j})^2] \tag{A.2}$$

$$q_{\alpha\beta}^{i,j} = n_\alpha^{i,j} n_\beta^{i,j} - \delta_{\alpha\beta}/2 \tag{A.3}$$

$$\mathcal{F}_{\mathrm{s}} = \frac{W\xi}{2} \sum_{i,j} \sum_{n=1}^{N} \left[\frac{1}{2} (\nabla_\alpha \phi_n^{i,j})^2 - (\nabla_\alpha \phi_n^{i,j})(\nabla_\beta \phi_n^{i,j}) q_{\alpha\beta}^{i,j} \right] \tag{A.4}$$

$$\begin{aligned} \frac{\partial \mathcal{F}}{\partial \theta^{i,j}} &= \frac{\partial \mathcal{F}}{\partial q_{\alpha\beta}^{i,j}} \frac{\partial q_{\alpha\beta}^{i,j}}{\partial \theta^{i,j}} = \frac{\partial \mathcal{F}}{\partial q_{xx}^{i,j}} \frac{\partial q_{xx}^{i,j}}{\partial \theta^{i,j}} + 2 \frac{\partial \mathcal{F}}{\partial q_{xy}^{i,j}} \frac{\partial q_{xy}^{i,j}}{\partial \theta^{i,j}} + \frac{\partial \mathcal{F}}{\partial q_{yy}^{i,j}} \frac{\partial q_{yy}^{i,j}}{\partial \theta^{i,j}} \\ &= 2 \sin \theta^{i,j} \cos \theta^{i,j} \left(\frac{\partial \mathcal{F}}{\partial q_{yy}^{i,j}} - \frac{\partial \mathcal{F}}{\partial q_{xx}^{i,j}} \right) + 2(\cos^2 \theta^{i,j} - \sin^2 \theta^{i,j}) \frac{\partial \mathcal{F}}{\partial q_{xy}^{i,j}} \end{aligned} \tag{A.5}$$

$$\frac{\partial \mathcal{F}}{\partial q_{\alpha\beta}^{i,j}} = \frac{\partial \mathcal{F}_{\mathrm{el}}}{\partial q_{\alpha\beta}^{i,j}} + \frac{\partial \mathcal{F}_{\mathrm{s}}}{\partial q_{\alpha\beta}^{i,j}} \tag{A.6}$$

$$\begin{aligned}\frac{\partial \mathcal{F}_{\mathrm{el}}}{\partial q_{\alpha\beta}^{i,j}} = \frac{K}{4l^2}\Bigg[&\left(1-\sum_{n=1}^{N}\phi_n^{i,j}\right)\cosh^{-2}\epsilon^{i,j}(4q_{\alpha\beta}^{i,j}-q_{\alpha\beta}^{i-1,j}-q_{\alpha\beta}^{i+1,j}-q_{\alpha\beta}^{i,j-1}-q_{\alpha\beta}^{i,j+1})\\ &+\left(1-\sum_{n=1}^{N}\phi_n^{i-1,j}\right)\cosh^{-2}\epsilon^{i-1,j}(q_{\alpha\beta}^{i,j}-q_{\alpha\beta}^{i-1,j})\\ &+\left(1-\sum_{n=1}^{N}\phi_n^{i+1,j}\right)\cosh^{-2}\epsilon^{i+1,j}(q_{\alpha\beta}^{i,j}-q_{\alpha\beta}^{i+1,j})\\ &+\left(1-\sum_{n=1}^{N}\phi_n^{i,j-1}\right)\cosh^{-2}\epsilon^{i,j-1}(q_{\alpha\beta}^{i,j}-q_{\alpha\beta}^{i,j-1})\\ &+\left(1-\sum_{n=1}^{N}\phi_n^{i,j+1}\right)\cosh^{-2}\epsilon^{i,j+1}(q_{\alpha\beta}^{i,j}-q_{\alpha\beta}^{i,j+1})\Bigg]\end{aligned} \tag{A.7}$$

$$\frac{\partial \mathcal{F}_{\mathrm{s}}}{\partial q_{\alpha\beta}^{i,j}} = -\frac{W\xi}{2}\sum_{n=1}^{N}\nabla_\alpha\phi_n^{i,j}\nabla_\beta\phi_n^{i,j} \tag{A.8}$$

$$\mathbf{f}_n^{\mathrm{PS}} = \frac{K}{4R_{\mathrm{c}}^2}\sum_{i,j}\frac{\partial\phi_n^{i,j}}{\partial\mathbf{R}_n}\tanh\epsilon^{(0)i,j} + W\xi\sum_{i,j}\frac{\partial(\nabla_\alpha\phi_n^{i,j})}{\partial\mathbf{R}_n}(\nabla_\beta\phi_n^{i,j})q_{\alpha\beta}^{(0)i,j}. \tag{A.9}$$

Appendix B. Numerical implementation for 2D smectic-C*

$$\mathcal{F}_{\mathrm{el}} = \frac{K}{2R_{\mathrm{c}}^2}\sum_{i,j}\left(1-\sum_{n=1}^{N}\phi_n^{i,j}\right)\tanh\epsilon^{i,j} \tag{B.1}$$

$$\epsilon^{i,j} = \frac{R_{\mathrm{c}}^2}{2l^2}[(n_\alpha^{i,j}-n_\alpha^{i-1,j})^2+(n_\alpha^{i+1,j}-n_\alpha^{i,j})^2+(n_\alpha^{i,j}-n_\alpha^{i,j-1})^2+(n_\alpha^{i,j+1}-n_\alpha^{i,j})^2] \tag{B.2}$$

$$\mathcal{F}_{\mathrm{s}} = W\xi\sum_{i,j}\sum_{n=1}^{N}[(\nabla\phi_n^{i,j})^2-|\nabla\phi_n^{i,j}|\nabla\phi_n^{i,j}\cdot\mathbf{n}^{i,j}] \tag{B.3}$$

$$\begin{aligned}\frac{\partial \mathcal{F}}{\partial\theta^{i,j}} &= \frac{\partial \mathcal{F}}{\partial n_\alpha^{i,j}}\frac{\partial n_\alpha^{i,j}}{\partial\theta^{i,j}} = \frac{\partial \mathcal{F}}{\partial n_x^{i,j}}\frac{\partial n_x^{i,j}}{\partial\theta^{i,j}} + \frac{\partial \mathcal{F}}{\partial n_y^{i,j}}\frac{\partial n_y^{i,j}}{\partial\theta^{i,j}}\\ &= -n_y^{i,j}\left(\frac{\partial \mathcal{F}_{\mathrm{el}}}{\partial n_x^{i,j}}+\frac{\partial \mathcal{F}_{\mathrm{s}}}{\partial n_x^{i,j}}\right)+n_x^{i,j}\left(\frac{\partial \mathcal{F}_{\mathrm{el}}}{\partial n_y^{i,j}}+\frac{\partial \mathcal{F}_{\mathrm{s}}}{\partial n_y^{i,j}}\right)\end{aligned} \tag{B.4}$$

$$\begin{aligned}\frac{\partial \mathcal{F}_{\mathrm{el}}}{\partial n_\alpha^{i,j}} = \frac{K}{2l^2}\Bigg[&\left(1-\sum_{n=1}^{N}\phi_n^{i,j}\right)\cosh^{-2}\epsilon^{i,j}(4n_\alpha^{i,j}-n_\alpha^{i-1,j}-n_\alpha^{i+1,j}-n_\alpha^{i,j-1}-n_\alpha^{i,j+1})\\ &+\left(1-\sum_{n=1}^{N}\phi_n^{i-1,j}\right)\cosh^{-2}\epsilon^{i-1,j}(n_\alpha^{i,j}-n_\alpha^{i-1,j})\\ &+\left(1-\sum_{n=1}^{N}\phi_n^{i+1,j}\right)\cosh^{-2}\epsilon^{i+1,j}(n_\alpha^{i,j}-n_\alpha^{i+1,j})\\ &+\left(1-\sum_{n=1}^{N}\phi_n^{i,j-1}\right)\cosh^{-2}\epsilon^{i,j-1}(n_\alpha^{i,j}-n_\alpha^{i,j-1})\end{aligned}$$

$$+\left(1-\sum_{n=1}^{N}\phi_n^{i,j+1}\right)\cosh^{-2}\epsilon^{i,j+1}(n_\alpha^{i,j}-n_\alpha^{i,j+1})\Bigg] \tag{B.5}$$

$$\frac{\partial\mathcal{F}_{\mathrm{s}}}{\partial n_\alpha^{i,j}}=-W\xi\sum_{n=1}^{N}|\nabla\phi_n^{i,j}|\nabla_\alpha\phi_n^{i,j} \tag{B.6}$$

$$\mathbf{f}_n^{\mathrm{PS}}=\frac{K}{2R_{\mathrm{c}}^2}\sum_{i,j}\frac{\partial\phi_n^{i,j}}{\partial\mathbf{R}_n}\tanh\epsilon^{(0)i,j}$$
$$+W\xi\sum_{i,j}\frac{\partial(\nabla_\alpha\phi_n^{i,j})}{\partial\mathbf{R}_n}\left(|\nabla\phi_n^{i,j}|n_\alpha^{i,j}+\frac{\nabla\phi_n^{i,j}\cdot\mathbf{n}^{i,j}}{|\nabla\phi_n^{i,j}|}\nabla_\alpha\phi_n^{i,j}\right). \tag{B.7}$$

References

[1] Russel W B, Saville D A and Schowalter W R 1995 *Colloidal Dispersions* (Cambridge: Cambridge University Press)
[2] Mostepanenko V M and Trunov N N 1997 *The Casimir Effect and its Application* (Oxford: Clarendon)
[3] Borštnik A, Stark H and Žumer S 1999 *Phys. Rev.* E **60** 4210
[4] Stark H 2001 *Phys. Rep.* **351** 387
[5] Terentjev E M 1995 *Phys. Rev.* E **51** 1330
[6] Ramaswamy S, Nityananda R, Raghunathan V A and Prost J 1996 *Mol. Cryst. Liq. Cryst.* **288** 175
[7] Ruhwandl R W and Terentjev E M 1997 *Phys. Rev.* E **56** 5561
[8] Stark H 1999 *Eur. Phys. J.* B **10** 311
Stark H, Stelzer J and Bernhard R 1999 *Eur. Phys. J.* B **10** 515
[9] Mondain-Monval O, Dedieu J C, Gulik-Krzywicki T and Poulin P 1999 *Eur. Phys. J.* B **12** 567
[10] Gu Y G and Abbott N L 2000 *Phys. Rev. Lett.* **85** 4719
[11] Poulin P, Stark H, Lubensky T C and Weitz D A 1997 *Science* **275** 1770
Poulin P, Cabuil V and Weitz D A 1997 *Phys. Rev. Lett.* **79** 4862
Poulin P and Weitz D A 1998 *Phys. Rev.* E **57** 626
[12] Ruhwandl R W and Terentjev E M 1997 *Phys. Rev.* E **55** 2958
[13] Lubensky T C, Pettey D, Currier N and Stark H 1998 *Phys. Rev.* E **57** 610
[14] Lev B I and Tomchuk P M 1999 *Phys. Rev.* E **59** 591
[15] Raghunathan V A, Richetti P and Roux D 1996 *Langmuir* **12** 3789
Raghunathan V A, Richetti P, Roux D, Nallet F and Sood K 2000 *Langmuir* **16** 4720
[16] Meeker S P, Poon W C K, Crain J and Terentjev E M 2000 *Phys. Rev.* E **61** R6083
Anderson V J, Terentjev E M, Meeker S P, Crain J and Poon W C K 2001 *Eur. Phys. J.* E **1** 11
Anderson V J and Terentjev E M 2001 *Eur. Phys. J.* E **1** 21
[17] Loudet J C, Barios P and Poulin P 2000 *Nature* **407** 611
[18] Yamamoto J and Tanaka H 2001 *Nature* **409** 321
[19] Nazarenko V G, Nych A B and Lev B I 2001 *Phys. Rev. Lett.* **87** 075504
[20] Yamamoto T, Yamamoto J, Lev B I and Yokoyama H 2002 *Appl. Phys. Lett.* **81** 2187
[21] Cluzeau P, Poulin P, Joly G and Nguyen H T 2001 *Phys. Rev.* E **63** 031702
[22] Patricio P, Tashinkevych M and Telo da Gama M M 2002 *Eur. Phys. J.* E **7** 117
[23] Petty D, Lubensky T C and Link D R 1998 *Liq. Cryst.* **25** 579
[24] Care C M, Halliday L, Good K and Lishchuk S V 2003 *Phys. Rev.* E **67** 061703
[25] Fukuda J 2004 *J. Phys.: Condens. Matter* **16** S1957
[26] Nakayama Y and Yamamoto R in preparation
[27] Kim K and Yamamoto R in preparation
[28] Billeter J L and Pelcovits R A 2000 *Phys. Rev.* E **62** 711
[29] Andrienko D, Germano G and Allen M P 2001 *Phys. Rev.* E **63** 041701
[30] Löwen H, Madden P A and Hansen J-P 1992 *Phys. Rev. Lett.* **68** 1081
Löwen H, Hansen J-P and Madden P A 1993 *J. Chem. Phys.* **98** 3275
[31] de Gennes P G and Prost J 1993 *The Physics of Liquid Crystals* 2nd edn (Oxford: Clarendon)
[32] Yamamoto R 2001 *Phys. Rev. Lett.* **87** 075502
[33] Tanaka H and Araki T 2000 *Phys. Rev. Lett.* **85** 1338
[34] Fukuda J and Yokoyama H 2001 *Eur. Phys. J.* E **4** 389
Fukuda J, Yoneya M and Yokoyama H 2002 *Phys. Rev.* E **65** 041709